Thin Solid Films 517 (2009) 1794–1798

Contents lists available at ScienceDirect

Thin Solid Films

journal homepage: www.elsevier.com/locate/tsf

Towards nanoporous polymer thin film-based drug delivery systems

Wei Yan [a], Vincent K.S. Hsiao [a], Yue Bing Zheng [a], Yasir M. Shariff [b], Tieyu Gao [c], Tony Jun Huang [a,*]

[a] Department of Engineering Science and Mechanics, The Pennsylvania State University, University Park, PA 16802, USA
[b] Mechanical Engineering Department, Taibah University, Madina, Saudi Arabia
[c] School of Energy and Power Engineering, Xi'an Jiaotong University, Xi'an, Shaanxi, 710049, China

ARTICLE INFO

Article history:
Received 26 February 2008
Received in revised form 6 August 2008
Accepted 12 September 2008
Available online 26 September 2008

Keywords:
Porous polymer films
Drug delivery
Rhodamine B
Ultrasound
Pulsatile release

ABSTRACT

A nanoporous polymer thin film has been developed as a potential platform for drug delivery. The film was fabricated by a light-induced polymerization process in which non-reactive solvent was first separated from photopolymer (dipentaerythritol penta-/hexa-acrylate as the monomer) and then removed from polymer via evaporation, yielding pores with diameters between 20 and 40 nm. Loading and release of Rhodamine B (drug model molecules) on both porous and non-porous thin films proved that nanopores enhanced the film's effectiveness in encapsulating and releasing the drug model molecules, which was attributed to the high surface-to-volume ratio of nanoporous film. Ultrasound-enhanced cumulative and pulsatile release revealed the advantages of ultrasound in controlled drug delivery.

1. Introduction

In recent years, nanoporous materials have attracted extensive interest because their high surface-to-volume ratios enhance their ability to adsorb molecules [1], lending them useful to drug delivery systems (DDS) [2]. Several materials, such as silicon [3–5], alumina [6], anodic alumina oxide [7], SiC [8], TiO_2 [9] and polymer [10], have been fabricated into nanoporous membranes and thin films for different DDS. In particular, nanoporous polymer materials are attractive for polymeric DDS due to their low cost, biocompatibility, and biodegradability [11–14]. Thus far, porous polymeric structures have been fabricated by methods like mold replication [15], colloidal lithography [16], interfacial polymerization [17], nanoimprinting [18], electrospinning [19], track etching [20], templating [21–23], holographic lithography [24–28] and self-assembly [29–31]. Despite these advances, the fabrication of nanoporous polymer thin films is complex and slow.

We fabricated a nanoporous polymer thin film by a simple, light-induced polymerization process. The photopolymer system contained acetone, a non-reactive solvent. During the photopolymerization process, the solvent phase separated from the photopolymer phase and formed nanoscale droplets. After the droplets of solvent evaporated, nanoscale air voids were left in the polymer structure. This nanoporous structure encapsulated many molecules of Rhodamine B, a dye commonly used as a drug model. The application of ultrasound to the film increased the rate at which it released Rhodamine B. Its ability to adsorb drug model molecules as well as the enhanced release of loaded molecules under ultrasound suggests that this nanoporous polymer thin film would be a potentially competent platform in DDS research.

2. Experimental details

2.1. Materials

Rose Bengal, *N*-phenylglycine (NPG, 95%), *N*-vinylpyrrolidinone (NVP, ≥99%), dipentaerythritol penta-/hexa-acrylate (DPHPA), 3-aminopropyltriethoxysilane (APTES, 99%), and acetone (Reagent-Plus, ≥9%) were purchased from Sigma-Aldrich. Liquid crystal (TL213) and Rhodamine B (Basic Violet 10) were obtained from EMD Chemicals, Inc. All chemicals were used without further purification. Uncoated glass slides and glass slides coated with indium tin oxide (ITO) were supplied by, respectively, VWR International and Delta Technologies, Ltd. All slides were cleaned by deionized (DI) water before experiments.

2.2. Fabrication of nanoporous and non-porous polymer thin films

A pre-polymer syrup was made with the following: 0.3 wt.% Rose Bengal, 0.8 wt.% NPG, 16.0 wt.% NVP, 18.0 wt.% liquid crystal TL213, 36.8 wt.% DPHPA, 21.4 wt.% acetone, and 6.7 wt.% APTES. The syrup was made homogeneous with a mixer and a sonicator (VWR International). 15 μL of pre-polymer syrup was deposited on a pre-

* Corresponding author.
E-mail address: junhuang@psu.edu (T.J. Huang).

0040-6090/$ – see front matter © 2008 Elsevier B.V. All rights reserved.
doi:10.1016/j.tsf.2008.09.080

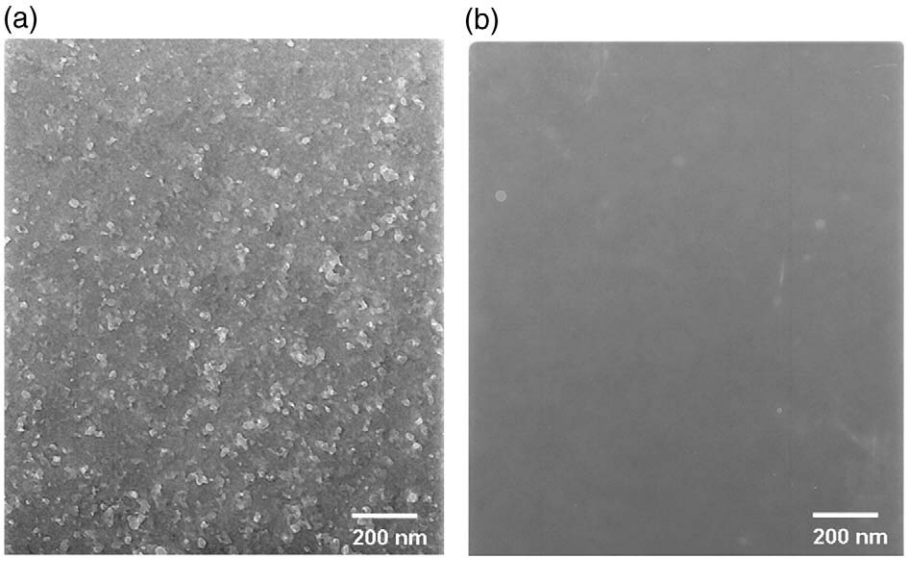

Fig. 1. Bright-field TEM cross-sectional morphologies of (a) nanoporous polymer thin film and (b) non-porous polymer thin film.

cleaned glass slide, which was covered immediately with an ITO-coated glass. The distance between the two glass slides was precisely controlled by adding microbeads (3 μm in diameter) at the edge of the syrup; controlling this distance defined the thickness of the polymer film to be fabricated. The syrup was exposed to an argon ion laser (Coherent Innova 300C, 514.5 nm, 1.92 W) which caused the syrup to polymerize. The exposure process lasted for approximately 1 min. Immediately following the polymerization, the sample was post-cured under white light for 24 h. After post-curing, the sample on the bare glass slide was separated from the ITO-coated cover slide; separation was readily achieved because of the poor adhesion between the sample and the ITO.

Acetone, a non-reactive solvent, was added to the polymer syrup in order to form nanopores in the thin film [24,25]. During the photopolymerization process, the solvent separated from the photopolymer to form nanoscale droplets. Upon the removal of ITO-coated cover slide, the droplets of solvent went through complete evaporation while nanoscale air voids were left in the polymer, making it nanoporous. Fig. 1a is a cross-sectional, bright-field transmission electron microscopy image of the nanoporous polymer thin films. The bright regions in micrograph were air voids, while the dark regions were the polymer. The nanopores were formed and uniformly distributed in the polymer matrix after the evaporation of the non-reactive solvent. The diameters of the pores were 20 to 40 nm, large enough to accommodate most drug molecules such as Rhodamine B (~1.6 nm in diameter) [32] and ibuprofen (~1.3 nm in diameter) [33]. For control experiments, a non-porous polymer was fabricated much like the porous polymer was, except that no acetone was added to the pre-polymer syrup. A non-porous structure formed because no solvent was present during post-curing (Fig. 1b).

2.3. Loading of Rhodamine B

The porous and non-porous polymeric samples were incubated in Rhodamine B solution (0.01 mg/mL) at room temperature for 5 h, and then rinsed with DI water to get rid of dye molecules that were loosely attached to the polymer. The samples were dried in the ambient environment. To determine the capacity of the samples to load drug model molecules, the absorption spectra of Rhodamine B solutions were measured with a spectrometer (HR4000, Ocean Optics, FL) after each of the above steps.

2.4. Release of Rhodamine B

Three experiments revealed how the nanopores affected the release of Rhodamine B: (1) natural release; (2) cumulative release with the application of ultrasound and without said application; and (3) pulsatile release with the periodic application of ultrasound. In all experiments, each Rhodamine B-loaded sample was placed upright in a micro-centrifuge tube (VWR International). The nanopores released the Rhodamine B when DI water of room temperature was added into the tube, immersing the whole sample. The release process was monitored by sequentially recording the absorption spectra of the Rhodamine B in DI water.

The details of the three experiments are as follows. (1) For natural release, each sample was immersed in 1 mL of DI water in a micro-centrifuge tube. The time to release was 120 min. Every 5 min, 0.5 mL of sample solution was removed from the tube in order to record its absorption spectra; it was then returned to the tube. (2) For cumulative release, the samples were immersed in DI water for 60 min in stilled tubes. The tubes were then subjected to ultrasound for another 60 min. The frequency of the ultrasound ranged from 38.5 to 40.5 kHz, and the average sonic power was 90 W. During the cumulative release process, 0.5 mL of DI water was removed from the tube every 10 min in order to record the absorption spectra of the water; it was then returned to the tube. (3) For pulsatile release, the samples were immersed in DI water within micro-centrifuge tubes for the first 5 min, followed by leaving the tubes in an ultrasonic bath for 5 min. These two steps constituted a natural/ultrasound-enhanced release period of 10 min. This period was repeated eight times in order to observe the release of Rhodamine B molecules under pulsatile ultrasound. The absorption spectra of the DI water were obtained every 5 min at the ultrasound on/off junctions.

3. Results and discussion

During the loading process, the Rhodamine B molecules were adsorbed inside the polymer thin films. This action decreased the concentration of Rhodamine B molecules in the solution, which

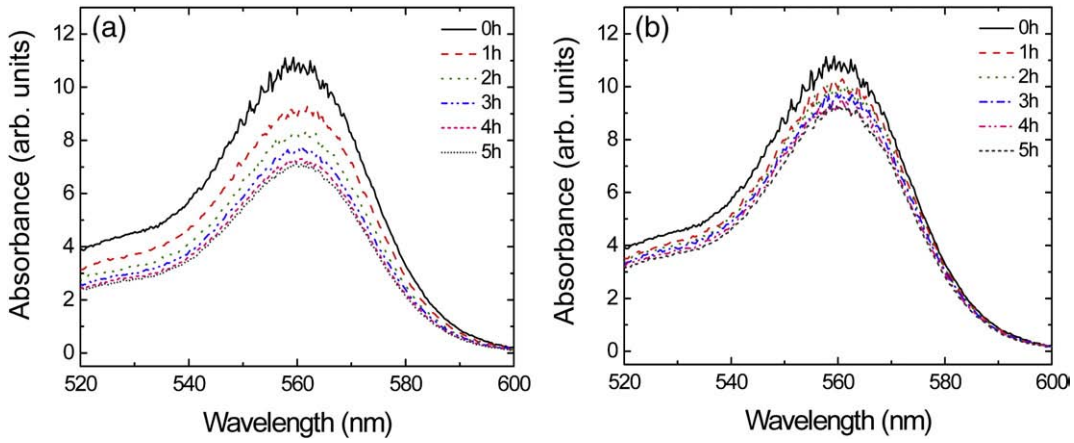

Fig. 2. Absorption spectra of Rhodamine B solution measured in (a) nanoporous polymer thin film and (b) non-porous polymer thin film, both during a 5-hour loading process. The concentrations of the Rhodamine B solution for the loading experiments were 0.01 mg/mL. The absorption spectra were measured every 1 h.

reduced the intensity of the solution's absorption spectra according to the Beer–Lambert law:

$$A = \alpha l c.$$

Here A is absorbance, α is the absorption coefficient of the absorber, l is the path length of light, and c is the concentration of the absorber. Per this law, the Rhodamine B-loading process was monitored by recording the absorption spectra and analyzing their peak intensities. The periodically recorded absorption spectra of the Rhodamine B solution are shown in Fig. 2. The nanoporous polymer (Fig. 2a) adsorbed about twice the amount of Rhodamine B molecules as the non-porous polymer did (Fig. 2b).

Fig. 3 depicts the time-dependent peak intensity for both nanoporous and non-porous samples. The nanoporous polymer had a higher adsorption rate of Rhodamine B molecules than the non-porous polymer did. The adsorption rate for both nanoporous and non-porous samples decreased as the loading process saturated.

The release of Rhodamine B from both nanoporous and non-porous polymeric samples was monitored. Fig. 4 shows the absorption spectra of the Rhodamine B solution during natural release by a nanoporous polymer thin film. The initial rapid increase in absorption intensity indicates that there was a burst release of Rhodamine B at the beginning of the release process. The burst release pattern was due to the drug model molecules being physical and chemical trapped [34,35]. The burst release was also consistent with the rapid adsorption of Rhodamine B molecules at the early stage of the loading process (Fig. 2). During the followed release process, the release rate gradually decreased until the Rhodamine B concentration in DI water reached equilibrium.

The time-dependent natural release profiles of the nanoporous and non-porous polymer thin films are shown in Fig. 5. Based on the calculation of the Rhodamine B solution's absorption intensity at the end of a 120-min release process, the average dye molecule-release rate of the nanoporous polymer was about twice that of the non-porous polymer. This result was consistent with the loading capacity experiment, in which the nanoporous polymer adsorbed about twice the amount of Rhodamine B molecules that the non-porous polymer did (Fig. 3). Furthermore, the nanoporous polymer exhibited a larger initial burst release, and its release rate started to decrease after around 60 min. The release appeared to reach equilibrium after about 100 min. In contrast, the non-porous polymer released dye molecules at an almost constant rate, and the initial burst effect was not as distinct. The difference between the natural release behavior of nanoporous and non-porous polymers indicated that the pore structure was a key factor in molecule encapsulation and release. During the loading process, the Rhodamine B molecules diffused through the nanoporous polymer thin film at a higher rate than through the non-porous polymer structure, and the diffusion rate decreased as the pores were occupied. During the release process, the diffusion kinetics exhibited a pattern similar to that for the loading but in the opposite direction. Nanoporous polymers are thus expected to

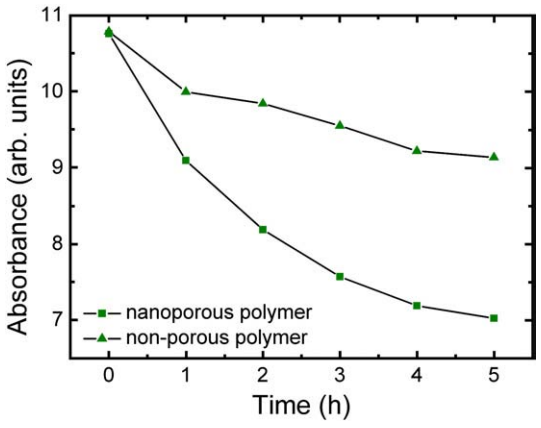

Fig. 3. Time-dependent absorption spectra of Rhodamine B solution within nanoporous and non-porous polymer thin films during a 5-hour loading process.

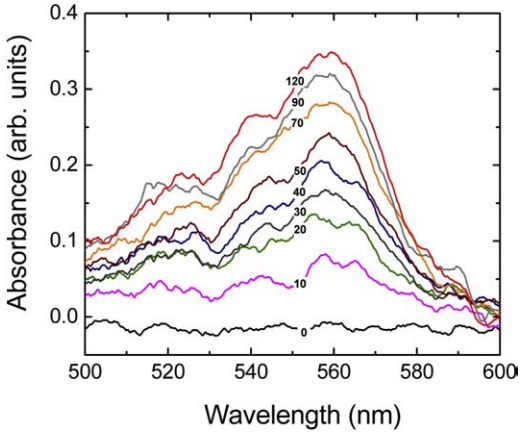

Fig. 4. Absorption spectra of Rhodamine B from a nanoporous polymer thin film during a 120-min natural release process.

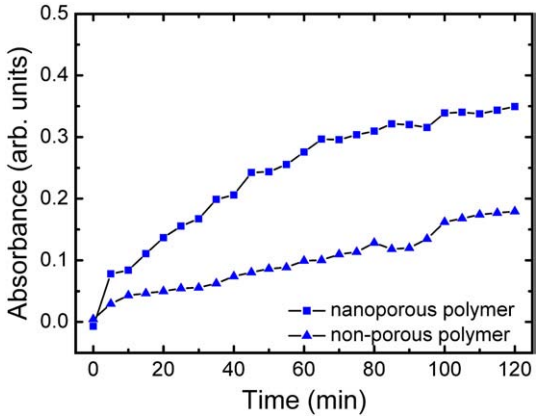

Fig. 5. Time-dependent absorption peak intensity of Rhodamine B for both nanoporous and non-porous polymer thin films. The release of Rhodamine B was observed by measuring absorption peak of Rhodamine B during the incubation of the thin film samples in 1 mL DI water.

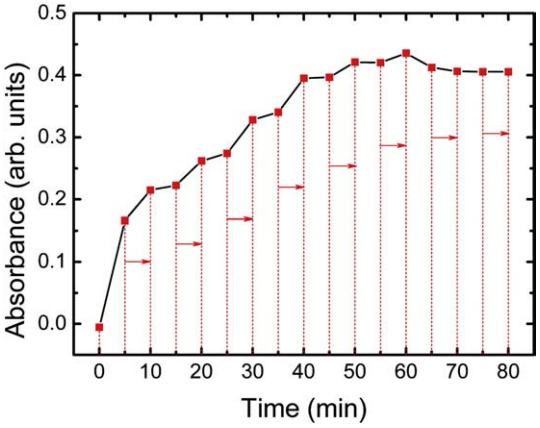

Fig. 7. Pulsatile release of Rhodamine B from a nanoporous polymer thin film. A 5-min natural release and a 5-min ultrasound-enhanced release alternated during the pulsatile release process (arrows show periods of ultrasound application).

be able to load and release larger amount of drugs than non-porous polymers can, making the former material useful in DDS.

Sustained or pulsatile ultrasound irradiation has been used to expedite the drug release process in a number of controlled drug delivery studies [36,37]. Ultrasound is a non-invasive way to deliver drugs to the innermost areas of the human body. To study how ultrasound causes Rhodamine B to be released from nanoporous polymer thin films, both cumulative and pulsatile release were examined. The cumulative release profiles of nanoporous and non-porous polymer thin films are shown in Fig. 6. In the first half of the cumulative release process, both films displayed behavior similar to that observed for natural release. When ultrasound was applied at 60 min into the cumulative release, the release rate for both polymer thin films drastically increased. At the end of ultrasonic application, the nanoporous polymer had released enough drug model molecules to reach equilibrium with the surroundings. The non-porous polymer showed a constant release rate much higher than that observed for the natural release process. This was because the ultrasound formed vapor-filled cavities (bubbles) in the polymers [38–43]. The acoustic energy generated extreme temperatures and pressures within a short time, thereby enhancing the desorption and the diffusion kinetics [37].

Fig. 7 shows how pulsatile release occurs for nanoporous polymer thin films under the periodic application of ultrasound. The release rate greatly increased when the sample was exposed to ultrasound, and it decreased when the ultrasound was stopped. The release profile reached equilibrium after 60 min. Both cumulative and pulsatile release experiments showed that ultrasound had an immediate influence on the release of molecules from nanoporous polymer thin films, making ultrasound an effective catalyst for controlled drug delivery in polymeric systems. By manipulating parameters such as frequency, power density, cycles, and duration of the ultrasound application, one can precisely control both the drug release rate and total dosage.

To establish this nanoporous polymer thin film system as an effective platform for implantable drug delivery devices, several critical challenges need to be addressed. First of all, the materials' biocompatibility has to be thoroughly investigated and optimized. Another logical step is to integrate the nanoporous polymer films with micro/nano-fluidic devices [44–48], biosensors [49–51], and other active nanostructures [52–61], thus realizing fully integrated, smart drug delivery system.

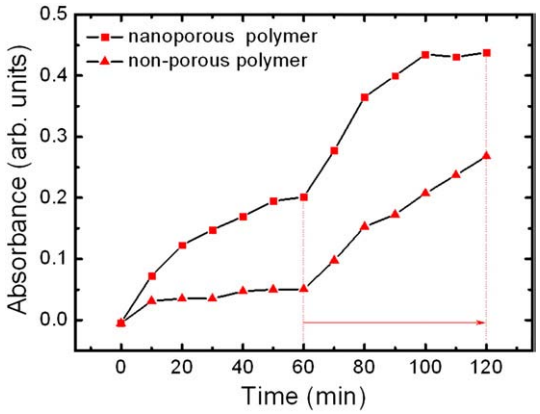

Fig. 6. Cumulative release of Rhodamine B from nanoporous and non-porous polymer thin films without and with ultrasound application. Ultrasound was applied from 60 min to 120 min into the release (the arrow shows the period of ultrasound application).

4. Conclusions

We developed a type of nanoporous polymer thin film for enhanced drug delivery. The addition of a non-reactive solvent into the pre-polymer syrup caused the formation of nanopores in the thin film. Compared with non-porous thin films, the porous polymeric structures exhibited much higher drug model loading and releasing rates. The release experiments showed that ultrasound is an effective and nondestructive means to trigger drug release, suggesting that our nanoporous polymeric structures can be used for the pulsatile release of drugs from implantable devices. Our future research will investigate and improve the biocompatibility and stability of the nanoporous polymer structures. With said structures, we will develop implantable drug carriers that operate by pulsatile release.

Acknowledgements

This work was supported by the National Science Foundation and the start-up fund provided by the Pennsylvania State University. Components of this work were conducted at the Pennsylvania State University node of the NSF-funded National Nanotechnology Infrastructure Network. The authors thank Thomas R. Walker for helpful discussion.

References

[1] G.A. Ozin, Adv. Mater. 4 (1992) 612.
[2] G.Q. Lu, X.S. Zhao, Nanoporous Materials — Science and Engineering, Imperial College Press, London, 2004.

[3] P.M. Sinha, G. Valco, S. Sharma, X. Liu, M. Ferrari, Nanotechnology 15 (2004) 585.
[4] S.L. Tao, T.A. Desai, Adv. Drug Deliv. Rev. 55 (2003) 315.
[5] J. Salonen, A.M. Kaukonen, J. Hirvonen, V-P. Lehto, J. Pharm. Sci. 97 (2008) 632.
[6] S. Kipke, G. Schmid, Adv. Funct. Mater. 14 (2004) 1184.
[7] H.-J. Kang, D.J. Kim, S.-J. Park, J.-B. Yoo, Y.S. Ryu, Thin Solid Films 515 (2007) 5184.
[8] A.J. Rosenbloom, D.M. Sipe, Y. Shishkin, Y. Ke, R.P. Devaty, W.J. Choyke, Biomed. Microdev. 6 (2004) 261.
[9] A.A. Ayon1, M. Cantu1, K. Chava, C.M. Agrawal, M.D. Feldman, D. Johnson, D. Patel, D. Marton, E. Shi, Biomed. Mater. 1 (2006) 11.
[10] S. Metz, C. Trautmann, A. Bertsch, Ph. Renaud, J. Micromechanics Microengineering 14 (2004) 324.
[11] S.W. Kim, R.V. Petersen, J. Feijen, in: J. Arien (Ed.), Drug Design, vol. 5, Academic Press, New York, 1980, p. 193.
[12] R. Langer, N.A. Peppas, Science 263 (1994) 1715.
[13] D.A.L. Van, T. McGuire, R. Langer, Nat. Biotechnol. 21 (2003) 1184.
[14] G.A. Hughes, Nanomedicine: Nanotechnol. Biol. Med. 1 (2005) 22.
[15] Y.Y. Li, F. Cunin, J.R. Link, T. Cao, R.E. Belts, S.H. Reiver, Science 299 (2003) 2045.
[16] M.J. Dalby, C.C. Berry, M.O. Riehle, D.S. Sutherland, H. Agheli, A.S.G. Curtisa, Exp. Cell Res. 295 (2004) 387.
[17] P. Couvreur, G. Barratt, E. Fattal, P. Legrand, C. Vauthier, Crit. Rev. Ther. Drug Carr. Syst. 19 (2002) 99.
[18] Y. Lu, S.C. Chen, Adv. Drug Deliv. Rev. 56 (2004) 1621.
[19] A. Frenot, I.S. Chronakis, Curr. Opin. Colloid Interface Sci. 8 (2003) 64.
[20] R.L. Fleischer, P.B. Price, R.M. Walker, Nuclear Tracks in Solids: Principles and Applications, University of California Press, Berkeley, 1975.
[21] H.-K. Lee, H. Lee, Y.H. Ko, Y.J. Chang, N.-K. Oh, W.-C. Zin, K. Kim, Angew. Chem. 113 (2001) 2741.
[22] Q. Li, J.F. Quinn, F. Caruso, Adv. Mater. 17 (2005) 2058.
[23] Y. Wang, F. Caruso, Chem. Mater. 18 (2006) 4089.
[24] V.K.S. Hsiao, T.C. Lin, G.S. He, A.N. Cartwright, P.N. Prasad, L.V. Natarajan, V.P. Tondiglia, T.J. Bunning, Appl. Phys. Lett. 86 (2005) 131113.
[25] V.K.S. Hsiao, W.D. Kirkey, F. Chen, A.N. Cartwright, P.N. Prasad, T.J. Bunning, Adv. Mater. 17 (2005) 2211.
[26] V.K.S. Hsiao, J.R. Waldeisen, Y.B. Zheng, P.F. Lloyd, T.J. Bunning, T.J. Huang, J. Mater. Chem. 17 (2007) 4896.
[27] J. Shi, V.K.S. Hsiao, T.J. Huang, Nanotechnology 18 (2007) 465501.
[28] J. Shi, V.K.S. Hsiao, T.R. Walker, T.J. Huang, Sens. Actuators, B 129 (2008) 391.
[29] Q.B. Meng, Z.Z. Gu, O. Sato, A. Fujishima, Appl. Phys. Lett. 77 (2000) 4313.
[30] J.D. Mendelsohn, C.J. Barrett, V.V. Chan, A.J. Pal, A.M. Mayes, M.F. Rubner, Langmuir 16 (2000) 5017.
[31] A. Fery, B. Scholer, T. Cassagneau, F. Caruso, Langmuir 17 (2001) 3779.
[32] F. Tsunomori, H. Ushiki, Phys. Lett. A 258 (1999) 171.
[33] P. Horcajadaa, C. Márquez-Alvarezb, A. Rámilaa, J. Pérez-Parientea, M. Vallet-Regí, Solid State Sci. 8 (2006) 1459.
[34] J. Andersson, J. Rosenholm, S. Areva, M. Lin den, Chem. Mater. 16 (2004) 4160.
[35] J.M. Xue, M. Shi, J. Control. Release 98 (2004) 209.
[36] A. Marin, Md. Muniruzzaman, N. Rapoport, J. Control. Release 71 (2001) 239.
[37] H.-J. Kim, H. Matsuda, H. Zhou, I. Honma, Adv. Mater. 18 (2006) 3083.
[38] J. Kost, Clin. Mater. 13 (1993) 155.
[39] A.C.R. Grayson, I.S. Choi, B.M. Tyler, P.P. Wang, H. Brem, M.J. Cima, R. Langer, Nat. Mater. 2 (2003) 767.
[40] C.S. Kwok, P.D. Mourad, L.A. Crum, B.D. Ratner, J. Biomed. Mater. Res. 57 (2001) 151.
[41] I. Lavon, J. Kost, J. Control. Release 54 (1998) 1.
[42] N.Y. Rapoport, D.A. Christensen, H.D. Fain, L. Barrows, Z. Gao, Ultrasonics 42 (2004) 943.
[43] S.B. Barnett, G.R. Ter Haar, M.C. Ziskin, W.L. Nyborg, K. Maeda, J. Bang, Ultrasound Med. Biol. 20 (3) (1994) 205.
[44] G.M. Whitesides, Nature 442 (2006) 368.
[45] X. Mao, J.R. Waldeisen, T.J. Huang, Lab Chip 7 (2007) 1260.
[46] X. Mao, J.R. Waldeisen, B.K. Juluri, T.J. Huang, Lab Chip 7 (2007) 1303.
[47] Y.B. Zheng, B.K. Juluri, T.J. Huang, Nanotechnology 18 (2007) 275706.
[48] J. Shi, X. Mao, D. Ahmed, A. Colletti, T.J. Huang, Lab Chip 8 (2008) 221.
[49] M.A. Cooper, Nat. Rev. Drug Discov. 1 (2002) 515.
[50] T.J. Huang, M. Liu, L.D. Knight, W.W. Grody, J.F. Miller, C.-M. Ho, Nucleic Acids Res. 30 (2002) e55.
[51] M. Gerard, A. Chaubey, B.D. Malhotra, Biosen. Bioelectr. 17 (2002) 345.
[52] V. Balzani, M. Venturi, A. Credi, Molecular Devices and Machines: a Journey Into the Nanoworld, Wiley-VCH, 2006.
[53] T.J. Huang, A.H. Flood, B. Brough, Y. Liu, P.A. Bonvallet, S. Kang, C.W. Chu, T.F. Guo, W. Lu, Y. Yang, IEEE T. Autom. Sci. Eng. 3 (2006) 254.
[54] Y.B. Zheng, T.J. Huang, A.Y. Desai, S.J. Wang, L.K. Tan, H. Gao, A.C.H. Huan, Appl. Phys. Lett. 90 (2007) 183117.
[55] T.J. Huang, MRS Bull. 33 (2008) 226.
[56] Y.B. Zheng, B.K. Juluri, X. Mao, T.R. Walker, T.J. Huang, J. Appl. Phys. 103 (2008) 014308.
[57] Y.B. Zheng, S.J. Chua, C.H.A. Huan, Z.L. Miao, J. Cryst. Growth 268 (2004) 369.
[58] B.K. Juluri, Y.B. Zheng, D. Ahmed, L. Jensen, T.J. Huang, J. Phys. Chem. C 112 (2008) 7309.
[59] Y.B. Zheng, S.J. Wang, C.H.A. Huang, Y.H. Wang, J. Non-Cryst. Solids 352 (2006) 2532.
[60] V.K.S. Hsiao, Y.B. Zheng, B.K. Juluri, T.J. Huang, Adv. Mater 20 (2008) 3528.
[61] T.J. Huang, B.K. Juluri, Nanomedicine 3 (2008) 107.